

Communication

Homogeneous Ice Nucleation Observed in Single Levitated Micro Droplets

B. Krämer¹, M. Schwell², O. Hübner¹, H. Vortisch¹,
T. Leisner¹, E. Rühl³, H. Baumgärtel²
and L. Wöste¹

(1) Institut für Experimentalphysik, Freie Universität Berlin, Arnimallee 14, D-14195 Berlin, Germany

(2) Institut für Physikalische und Theoretische Chemie, Freie Universität Berlin, Takustr. 3, D-14195 Berlin, Germany

(3) Fachbereich Physik, Universität Osnabrück, Barbarastr. 7, D-49069 Osnabrück, Germany

Key Words: Aerosols / Droplets / Light Scattering / Nucleation / Water

Homogeneous ice nucleation rates in single isolated micro droplets of water are determined under various atmospheric conditions inside an electrodynamic Paul-trap. The droplet size is measured by angle-resolved detection of the scattered light from a Helium-Neon laser. The freezing process is detected by a sudden change of the depolarization ratio which is an indication for the formation of non spherical particles.

The experimentally determined homogeneous ice nucleation rates J_{LS} are $J_{LS} = (2.2 \pm 0.4) \cdot 10^8 \text{ cm}^{-3} \text{ s}^{-1}$ at $T = (-37.2 \pm 0.15)^\circ\text{C}$ and $J_{LS} = (5.6 \pm 1.0) \cdot 10^7 \text{ cm}^{-3} \text{ s}^{-1}$ at $T = (-37.7 \pm 0.15)^\circ\text{C}$.

These values are much more precise as determined by measurements inside a cloud expansion chamber. The method of single particle observation eliminates complications arising from these nucleation rate measurements. The results underline the theory that one single ice germ of certain size is sufficient to induce the freezing of the whole droplet. The depolarization ratio of the scattered intensity in the parallel and perpendicular polarization plane I_{\parallel}/I_{\perp} from the frozen particles exhibits a broad distribution with a mean value of $I_{\parallel}/I_{\perp} = 0.3$.

Introduction

The physical and chemical properties of aerosol particles are of great scientific interest because of their important role in atmospheric processes, like stratospheric ozone depletion [1], cloud condensation mechanisms [2] and climate change [3]. Most work has been performed so far in field measurements where the properties of aerosols were determined by means of in situ and remote sensing experiments [4]. Laboratory experiments have mainly concentrated on freezing and melting of macroscopic samples consisting of binary and ternary mixtures [5], vapor pressure experiments [6], and more recently on single levitated particles [7]. Various levitation techniques are known to be suitable for investigations of single particles, such as optical, acoustical, and electrodynamic levitation. The technique of electrodynamic levitation is well established and provides a powerful tool for the investigation of such particle properties which are inaccessible to bulk measurements.

Our apparatus was developed to investigate the physical and chemical behavior of these particles. It allows to study their properties as a function of parameters like temperature, pressure, composition of the surrounding gas phase, and of the particle itself. From these one can obtain insight into processes and properties related to the stored particles.

For example there are to date no direct measurements on the homogeneous ice nucleation rate in single, isolated micron-sized water droplets. The existing experimentally determined values were derived by methods such as expansion cloud chamber experiments with ensembles of drops [8,9], calorimetric measurements on water-oil emulsions [10], remote sensing (LIDAR) and in-situ observations of cirrus cloud droplets in conjunction with a mixed phase hydrometer growth model [11].

It has been pointed out recently that there is a need in the accurate determination of homogeneous ice nucleation rates since this mechanism plays a fundamental role in the formation of cirrus cloud droplets. It is therefore closely related to climate modeling [12]. In this paper we present the first results on the direct determination of homogeneous ice nucleation rates determined by observing levitated single aerosol particles.

Experimental

Fig. 1 shows a schematic diagram of the experimental setup. Liquid water droplets are injected into a Paul-trap by using a commercially available, piezo-driven particle generator (Microdrop) which is equipped with a 40 μm diameter nozzle. For this triply distilled water was filtered through 0.2 μm pore-size nylon-membrane filters (Roth). The quadrupole trap consists of a horizontally fixed, ring-shaped electrode and two endcap electrodes. The ring-shaped electrode carries an AC voltage which is adjustable from 0.5 up to 6 kV at frequencies between 10 and 1000 Hz. The gravitational force of a trapped particle is compensated by a DC voltage on the endcap electrodes. All electrodes have hyperbolically shaped surfaces.

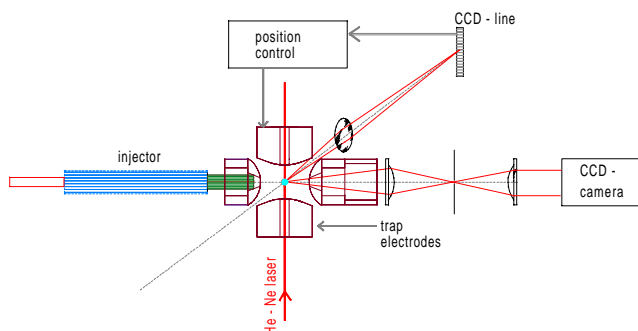


Fig1: Schematic diagram of the experimental setup.

The particle is illuminated with light from a linearly-polarized Helium-Neon laser operating at $\lambda = 632.8 \text{ nm}$. The scattered light is split into the parallel and the perpendicular polarization direction using a birefringent crystal (not shown in Fig. 1). It is then detected with a CCD-camera having 512 x 784 pixels. This covers an angular range between 80° and 100° relative to the incident laser beam with an angular resolution of 0.03° . The camera operates at a repetition rate of 25 Hz. Images of the

scattered light are

stored on a video recorder and are subsequently digitized for further analyzing. The particle evaporates during its observation leading to a non-constant position of the droplet inside the trap. In order to compensate for this, the vertical position of the particle is permanently controlled by detecting the scattered light with an additional CCD-line having 256 pixels. From this position measurement a control voltage is applied to the endcap electrodes to center the particle in the trap.

The trap is located in a chamber, which can be cooled with liquid nitrogen. The chamber can be evacuated to pressures of 10-6 mbar or it can be filled with gas mixtures up to 2 bar. The temperature is measured at different locations in the trap using a Pt-100 resistor and thermocouples. They are calibrated with ice/water and dry-ice/acetone mixtures. The temperature is stabilized with a process-controller. The liquid nitrogen cooled trap chamber is surrounded by another vacuum vessel which provides the necessary thermal insulation. The experiments were generally carried out by using Helium with an ambient pressure of about 500 mbar in the trap chamber.

Results and Discussion

Fig. 2a shows a typical scattering pattern of a liquid water droplet recorded with a CCD-camera. It exhibits a sequence of bright and dark stripes which are due to Mie scattering of spherical particles. The size of this particle is evidently greater than the wavelength of the illuminating radiation (632.8 nm). The observed stripe pattern strongly depends on the droplet size and the corresponding refractive index. The recorded scattering patterns are analyzed by using classical Mie theory, providing the size and refractive index within an error limit of 1%. Fig. 2b shows the scattered light of the same particle after freezing. The initially quite regular stripe pattern exhibited by the liquid droplet is now severely disturbed due to the enhanced surface roughness of the newly frozen particle. However, stripes are still visible

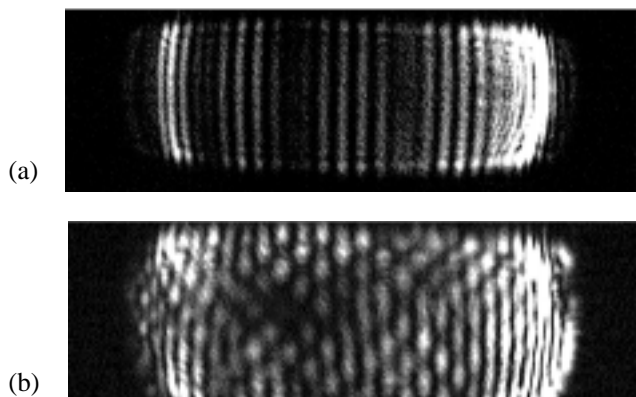


Fig. 2

Scattering pattern of a single water droplet ($T_{\text{chamber}} = -25^{\circ}\text{C}$, $p_{\text{chamber}} = 500 \text{ mbar}$) (a) liquid droplet; (b) after freezing of the droplet. The droplet has a diameter of 50 μm . Shown is the parallel polarization plane.

at the same positions as prior to freezing. This indicates that the frozen particle remains in its spherical shape. The observed structure is regular showing reproducibly hexagonal patterns. This suggests, that at least the surface of the particle contains crystalline regions. We have however also observed frozen particles without any characteristic stripe pattern. This suggests that the crystallization process completely destroyed the spherical shape of the droplet. Few particles even exploded while freezing leaving behind charged smaller fragments. Fig. 3 shows the analysis of the depolarization ratio I_s/I_p of the scattered light for 200 frozen ice particles in the scattering direction from 80° to 100° . All particles have been stored as liquid droplets in the trap and froze during observation. I_p (I_s) denotes the intensity of the scattered light with parallel (perpendicular) polarization with respect to the incoming light. Most of the frozen particles have a depolarization ratio ranging between 0.1 and 0.5 with a mean value of 0.3. We suggest that this distribution does not differ significantly when the light is detected in the backward scattering direction. In remote sensing experiments, the detection of frozen particles in the atmosphere is often done by analyzing the depolarization ratio of the backward scattered light (LIDAR, see for example ref. [11]). It is helpful for the analysis of the LIDAR-data to know the distribution of the depolarization ratio of frozen ice particles. We suggest that the mean depolarization ratio of atmospheric ice particles formed by diffusional growth is higher than that of ice particles which have been liquid before freezing. From that one might get new insight in the glaciation process of cirrus clouds. Furthermore, we did not find ice particles with a depolarization ratio below 5%. Since the detection sensitivity for the depolarization ratio in LIDAR measurements is about 1%, we can conclude that all frozen ice particles can be detected with this technique.

For measurements of the homogeneous nucleation rate of ice, the inner chamber is cooled to temperatures below -30°C while the temperature of the injector reservoir is constantly kept at $+20^{\circ}\text{C}$. The pressure of the Helium gas

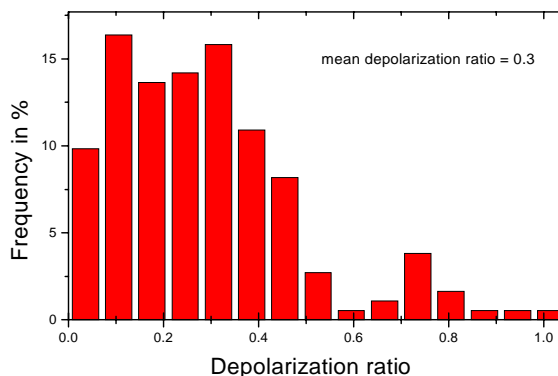


Fig 3:

Percentage of frozen particles with a certain depolarization ratio. The total number of observed particles is 200.

in the trap chamber is lowered to about 500 mbar in order to keep the impact of thermal fluctuations on the particle as small as possible. The water droplets are injected into the trap where they rapidly cool to the ambient temperature. At these conditions a trapped droplet vaporizes within 10-20 seconds at -30°C . The mixing ratio of H_2O in the inner chamber ranges from 100-150 ppm at a total pressure of 500 mbar.

At a temperature of $T = -30^{\circ}\text{C}$, none of the observed droplets has frozen within the evaporation time. On the other hand, in all cases instantaneous freezing is observed if the temperature is below -38.5°C . Thus it can be assumed that the cooling rate of the droplet is faster than the time resolution of the video camera. Furthermore we conclude that trapped liquid droplets are supercooled and that they are always, even though they evaporate, in good thermal equilibrium with the surrounding gas atmosphere. This assumption is in agreement with gas kinetic considerations: Applying Fick's first law to the diffusion of heat into a $50\ \mu\text{m}$ diameter water droplet in a 0.5 bar Helium atmosphere which is exposed to a temperature gradient of 40 K, one obtains a cooling rate of $\sim 7\ \text{K/ms}$ assuming infinitely fast thermal diffusion inside the droplet. The consumption of latent heat by an evaporating droplet is estimated to cool the droplet by about $0.02\ \text{K/ms}$ considering the observed evaporation speed. It is therefore considerably lower than the rate of heat transport into the droplet, suggesting that the temperature of the droplet during evaporation is in equilibrium with the surrounding atmosphere.

The scattered light of one droplet is observed until it either evaporates or freezes. A frozen particle is unambiguously identified by the sudden change in the scattering behavior. The time scales of the crystallization process cannot be precisely studied with the present setup. They are faster than the recording frequency of 25 Hz.

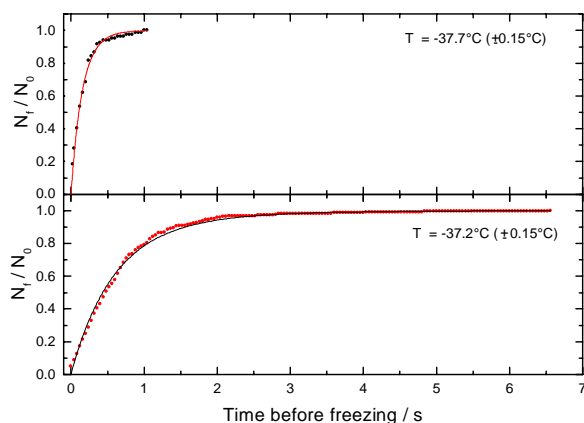


Fig. 4: Freezing probability of liquid water droplets at the temperature $T = -37.2 \pm 0.2^{\circ}\text{C}$ ($N_0 = 220$) and $T = -37.7 \pm 0.2^{\circ}\text{C}$ ($N_0 = 82$).

N_0 is the total number of observed droplets. N_f is the fraction of frozen droplets. $p_{\text{chamber}} = 500\ \text{mbar}$; dots: experimental data; solid line: fit according to Eq. (1). Further details: see text.

Typically 100-300 droplets are investigated in order to obtain sufficient statistics on the freezing behavior at a given temperature.

Fig. 4 shows the freezing probability as a function of time at the temperature $T = -37.2^{\circ}\text{C}$. The experimental data are fitted by varying the nucleation rate $J_{\text{LS}}(T)$ in equation (1) [2]:

$$N_f(t)/N_0 = 1 - \exp(-V_d(t) \cdot J_{\text{LS}}(T) \cdot t) \quad \text{with}$$

$$V_d(t) = 4\pi/3(r_0 - (v_e \cdot t)/2)^3 \quad (1)$$

$N_f(t)$ is the total number of frozen particles observed after a time t at a fixed temperature, N_0 denotes the total number of single particles, which have been measured. J_{LS} is the homogeneous nucleation rate of the liquid to solid phase transition. $V_d(t)$ is the droplets mean volume and v_e the evaporation speed, r_0 is the initial radius of the observed droplet. For some drops, the radii were determined as a function of the evaporation time by analyzing the Mie-structure of the recorded scattered light. This evaluation shows, that the initial radius r_0 varies only by about 3 % from one droplet to another which is due to irregularities in the injection process. The evaporation speed v_e of the droplets is nearly constant during the measurements and the radius decay was determined to $0.7 \cdot 10^{-4}\ \text{cm/s}$ at $T = -37.2^{\circ}\text{C}$. The absolute error of the nucleation time is on the order of 0.05 s. Equation (1) is derived assuming that only one ice germ of certain size inside the liquid droplet is sufficient for the crystallization of the whole particle and the nucleation rate for the ice germ formation depends only on the ambient temperature [2]. The good agreement between this theory and our experimental data gives evidence for the homogeneous ice nucleation process.

Fig. 5 shows J_{LS} values as a function of temperature. The values determined in this work are plotted together with

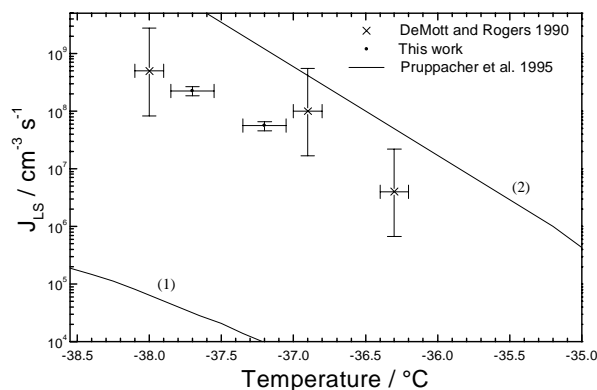


Fig.5: Homogeneous nucleation rates of ice as a function of temperature. The solid curves (1) and (2) are adapted from ref. [12]. (1) represents the classical nucleation theory and (2) an extension of the

classical theory based on recently experimentally determined thermodynamic values on supercooled water [13,14].

the recently published theoretical results given by Pruppacher [12] and experimental J_{LS} values determined in an expansion cloud chamber experiment of DeMott and Rogers [9]. The solid curve (1) represents the result of classical nucleation theory, while curve (2) includes newly determined values for the specific heat [13] and density of supercooled water [14].

The determination of the homogeneous nucleation rate in single levitated water droplets exhibits two advantages compared to former experimental techniques. First, this method allows to measure exactly the size of the droplet at any time until it freezes. The volume for the ice germ formation is therefore exactly known. Furthermore the time until a droplet freezes can be detected with high precision. This means that high accuracy is reachable for the determination of the ice nucleation rate. Second, any other influences on the ice germ formation can be ruled out since the particle is confined without any wall contact in the trap and the water used for the droplet formation can be cleaned to a sufficient extent.

Our experimentally determined nucleation rates of ice are well within the error limits of those obtained from expansion cloud chamber measurements (cf. Fig. 5) [9]. In these experiments condensation nuclei are necessary to produce the water droplets in the expansion cloud chamber. However, measurements on single levitated droplets derive homogeneous nucleation rates without any nucleation nuclei. In addition, the homogeneous nucleation rates of water are two orders of magnitude more precise compared to the expansion cloud chamber technique.

Conclusion

The measurement of homogeneous nucleation rates of single levitated water droplets gives precise values for the ice germ formation in supercooled water. Since the particle is levitated without contact to any wall in the trap and the water can be cleaned to a sufficient extent, restrictions as in other experimental techniques are avoided.

The distribution of the depolarization ratio for frozen water droplets could be determined. These values are important for the evaluation of the amount and genesis of frozen ice particles in the atmosphere with remote sensing techniques.

The results underline the theory that one single ice germ of critical size is sufficient to induce the freezing of the whole droplet.

We have determined homogeneous ice nucleation rates for two different temperatures. Work is in progress to measure J_{LS} values for higher temperatures using an injector to produce droplets of bigger size. With these measurements we will be able to derive the activation energy for the transfer of water molecules across the ice-water interface with high accuracy.

The authors would like to thank Stefanie Meilinger, Thomas Koop, Ulrich Krieger and Thomas Peter for helpful discussions and communicating results prior to publication as well as Nils Damaschke for providing the fast Mie scattering code. Financial support is gratefully acknowledged by the Kommission für Forschung und Nachwuchs (FNK) of the Freie Universität Berlin.

References

- [1] (a) M.A. Tolbert, *Science*, 264, 527 (1994);
(b) A.R. MacKenzie, M. Kulmala, A. Laaksonen, T. Vesala, *J. Geophys. Res.*, 100, 11275 (1995);
(c) T. Koop, K. Carslaw, *Science*, 272, 1638 (1996).
- [2] H.R. Pruppacher, J.D. Klett, "Microphysics of clouds and precipitation", Reidel: Dordrecht (1978).
- [3] S.E. Schwartz, M.O. Andreae, *Science*, 272, 1121 (1996).
- [4] (a) M. Del Guasta, M. Morandi, L. Stefanutti, B. Stein, J. Kolenda, P. Rairoux, J.P. Wolf, R. Matthey, E. Kyro, *Geophys. Res. Lett.*, 21, 1339 (1994);
(b) R.G. Grainger, A. Lambert, C.D. Rodgers, F.W. Taylor, T. Deshler, *J. Geophys. Res.*, 100, 16507 (1995).
- [5] (a) T. Othake, *Tellus*, 45B, 138 (1993);
(b) K.D. Beyer, *Geophys. Res. Lett.*, 21, 871 (1994);
(c) T. Koop, U.M. Biermann, W. Raber, B.P. Luo, P.J. Crutzen, T. Peter, *Geophys. Res. Lett.*, 22, 917 (1995).
- [6] R. Zhang, P.J. Wooldridge, M.J. Molina, *J. Phys. Chem.*, 97, 8541 (1993).
- [7] I.N. Tang, K.H. Fung, D.G. Imre, H.R. Munkelwitz, *Aerosol Sci. Technol.*, 23, 443 (1995).
- [8] D.E. Hagen, R.J. Anderson, J.L. Kassner jr., *J. Atmos. Sci.*, 38, 1236 (1981).
- [9] P.J. DeMott, D.C. Rogers, *J. Atmos. Sci.*, 47, 1056 (1990).
- [10] P. Taborek, *Phys. Rev. B*, 32, 5902 (1985).
- [11] K. Sassen, G.C. Dodd, *J. Atmos. Sci.*, 45, 1357 (1988).
- [12] H.R. Pruppacher, *J. Atmos. Sci.*, 52, 1924 (1995).
- [13] C.A. Angell, M.O. Guni, W.J. Sichina, *J. Phys. Chem.*, 86, 998 (1982).
- [14] D.E. Hare, C.M. Sorensen, *J. Chem. Phys.*, 87, 4840 (1987).

(Received: September 12 1996
final version October 15, 1996)

E 9367